Phosphoinositide 3-kinase signaling is critical for ErbB3-driven breast cancer cell motility and metastasis

Tatiana Smirnova, Ph.D.[1], **Zhen Ni Zhou, M.S.**[1], **Rory J. Flinn, Ph.D.**[2], **Jeffrey Wyckoff, B.A.**[1,3], **Pamela J. Boimel, M.S.**[1], **Maria Pozzuto, B.A.**[4], **Salvatore J. Coniglio, Ph.D.**[1], **Jonathan M. Backer, M.D.**[2], **Anne R. Bresnick, Ph.D.**[4], **John S. Condeelis, Ph.D.**[1,3], **Nancy E. Hynes, Ph.D.**[5], and **Jeffrey E. Segall, Ph.D.**[1,3]

[1]Department of Anatomy and Structural Biology, Maulbeerstrasse 66, CH-4058 Basel, Switzerland [2]Department of Molecular Pharmacology, Maulbeerstrasse 66, CH-4058 Basel, Switzerland [3]Gruss Lipper Center for Biophotonics, Maulbeerstrasse 66, CH-4058 Basel, Switzerland [4]Department of Biochemistry, Maulbeerstrasse 66, CH-4058 Basel, Switzerland [5]Friedrich Miescher Institute for Biomedical Research, Maulbeerstrasse 66, CH-4058 Basel, Switzerland

Abstract

Many malignancies show increased expression of the EGF receptor family member ErbB3 (HER3). ErbB3 binds beta-1 (HRGβ1), and forms a heterodimer with other ErbB family members, such as ErbB2 (HER2) or EGFR (HER1), enhancing phosphorylation of specific C terminal tyrosine residues and activation of downstream signaling pathways. ErbB3 contains six YXXM motifs that bind the p85 subunit of PI3-kinase. Previous studies demonstrated that overexpression of ErbB3 in mammary tumor cells can significantly enhance chemotaxis to HRGβ1 and overall metastatic potential. We tested the hypothesis that ErbB3-mediated PI3-kinase signaling is critical for heregulin-induced motility, and therefore crucial for ErbB3-mediated invasion, intravasation and metastasis. The tyrosines in the six YXXM motifs on the ErbB3 C-terminus were replaced with phenylalanine. In contrast to overexpression of the wild-type ErbB3, overexpression of the mutant ErbB3 did not enhance chemotaxis towards HRGβ1 *in vitro* or *in vivo*. We also observed reduced tumor cell motility in the primary tumor by multiphoton microscopy, as well as a dramatically reduced ability of these cells to cross the endothelium and intravasate into the circulation. Moreover, while mutation of the ErbB3 C-terminus had no effect on tumor growth, it had a dramatic effect on spontaneous metastatic potential. Treatment with the PI3-kinase inhibitor PIK-75 similarly inhibited motility and invasion *in vitro* and *in vivo*. Our results indicate that stimulation of the early metastatic steps of motility and invasion by ErbB3 requires activation of the PI3-kinase pathway by the ErbB3 receptor.

Corresponding Author: Jeffrey E. Segall, Albert Einstein College of Medicine, 1300 Morris Park Avenue, Bronx, NY 10801. Phone: 718-678-1109; Fax: 718-678-1019; jeffrey.segall@einstein.yu.edu.

INTRODUCTION

The epidermal growth factor receptor (EGFR) family has been a major target of anticancer therapy development (Di Cosimo and Baselga, 2010). Its members can contribute to a wide range of cell phenomena including proliferation, apoptosis, survival, invasion, and differentiation in both normal and neoplastic cells. Members of this family include the epidermal growth factor receptor (EGFR or ErbB1), ErbB2 (Her2/neu), ErbB3 and ErbB4 (Burgess, 2008). ErbB1 and ErbB2 have been most thoroughly studied, with a number of different inhibitors developed in hopes of identifying a treatment that will improve patient survival. However, the functions of ErbB1 and ErbB2 can be dependent upon ErbB3 expression through heterodimerization, and this dependency has repercussions for how tumors may respond to inhibitor treatment (Baselga and Swain, 2009). In NSCLCs that are driven by activating EGFR mutations, high ErbB3 expression is an indicator for gefitinib sensitivity (Engelman et al., 2005; Fujimoto et al., 2005), suggesting that ErbB1/ErbB3 heterodimers may be critical oncogenic units in these tumors. Indeed the development of resistance to EGFR inhibitors in NSCLCs can occur through restoration of ErbB3 activation by upregulation of c-Met (Engelman et al., 2007). In breast cancer, the ErbB2/ErbB3 heterodimer can also form a potent oncogenic unit (Amin et al.; Holbro et al., 2003). In mouse models where ErbB2 overexpression in the mammary gland drives tumor formation, ErbB3 expression and phosphorylation are upregulated (Schade et al., 2007; Siegel et al., 1999). Increased ErbB3 expression correlates with higher hazard ratios for reduced survival of breast cancer patients (Chiu et al.; Sassen et al., 2008).

ErbB3 binds heregulin beta-1 (HRGβ1), but is unable to stimulate downstream signaling on its own as it has a defective kinase domain; however, heterodimerization with another ErbB family member, such as ErbB2 or EGFR, permits tyrosine phosphorylation of the ErbB3 C-terminal domain (Campbell et al., 2010). Downstream signaling from the ErbB receptors includes the activation of a number of pathways, including the PI3-kinase pathway. ErbB3 contains six YXXM motifs that bind the p85 subunit of PI3-kinase (Fiddes et al., 1998; Hellyer et al., 2001; Prigent and Gullick, 1994; Vijapurkar et al., 2003), emphasizing the potential importance of ErbB3 in PI3-kinase activation. In NIH 3T3 cells, mutation of specific tyrosines in the ErbB3 C-terminus uncouples ErbB3 from PI3-kinase, with a strong effect on HRGβ1-stimulated cell transformation and mitogenic responses (Hellyer et al., 2001; Vijapurkar et al., 2003). Previous studies from our laboratory demonstrated that in MTLn3 mammary tumor cells, ErbB3 expression significantly enhances the chemotactic response and *in vivo* invasion towards HRGβ1, as well as greatly increases metastatic potential without affecting primary tumor growth rate (Hernandez et al., 2009a; Zhang et al., 2006). Thus this model provides a valuable tool for examining how ErbB3 signaling affects metastatic properties beyond the enhancement of cell survival. PI3-kinase signaling via ErbB3 has the potential to modulate actin cytoskeleton rearrangement, thus influencing

motility and chemotaxis (Adam et al., 1998; Cain and Ridley, 2009; Chausovsky et al., 2000).

In this paper we tested the hypothesis that the PI3-kinase signaling pathway coupled to ErbB3 is critical for motility, and therefore crucial for invasion, intravasation and metastasis. We created a version of the human ErbB3 receptor in which all six tyrosine residues responsible for binding the p85 subunit of PI3-kinase were replaced with phenylalanine, and evaluated breast cancer cell lines stably expressing either the wild-type ErbB3 or the mutant ErbB3 receptor. Our data revealed that mutation of the PI3K binding sites blocked a number of responses that are enhanced by overexpression of wild-type ErbB3. These include enhanced chemotaxis towards HRGβ1 *in vitro* and *in vivo*, increased tumor cell motility in the primary tumor, and increased transendothelial migration, intravasation, and metastasis. Taken together, our results demonstrate that coupling of the PI3-kinase pathway to ErbB3 is essential during the initial steps of breast cancer metastasis.

RESULTS

The PI3-kinase binding sites are required for HRGβ1-stimulated ErbB3 p85 phosphorylation, p85 association, chemotaxis and invasion

We created a version of the human ErbB3 receptor in which the tyrosines for all six YXXM motifs responsible for binding the p85 subunit of PI3-kinase were replaced with phenylalanine by site-directed mutagenesis. We then generated stable transductants of MTLn3 cells with the empty vector pLXSN (pLXSN), the wild-type human ErbB3 receptor (ErbB3WT), or the human ErbB3 receptor mutated in all six PI3-kinase binding sites (ErbB3-Mutant). Surface overexpression levels of the ErbB3WT and ErbB3-Mutant constructs were similar (Figure 1A). The endogenous rat ErbB3 was reduced using a rat-specific shRNA. All of the cell lines also stably expressed GFP. To measure ErbB3-Mutant and WT signaling activity, starved cultures were stimulated with HRGβ1, and ErbB3 was immunoprecipitated from MTLn3 ErbB3WT and ErbB3-Mutant cell lysates. ErbB3 signaling activity and coupling to the PI3K pathway was assessed by measuring ErbB3 immunoprecipitates (IP) for tyrosine phosphorylation (PTyr) and p85α association. ErbB3 IPs from HRGβ1-stimulated ErbB3WT cells had high levels of PTyr and complexed p85α, while ErbB3 IPs from ErbB3-Mutant cells had very low levels of PTyr and little or no associated p85α (Figure 1B). We then tested whether decreased signaling through PI3K had an effect on HRGβ1-induced chemotaxis (Figure 1C). ErbB3WT cells showed dramatically enhanced chemotaxis to HRGβ1 compared to the control pLXSN cell line. In contrast, ErbB3-Mutant cells were similar to control cells, indicating that removal of the PI3-kinase binding sites completely blocks chemotactic responses driven by HRGβ1. Chemotaxis in response to insulin did not show differences between ErbB3WT and ErbB3-Mutant cells (Supplementary Figure 1). We also measured tumor cell invasiveness using Matrigel-coated transwells. We found that HRGβ1 significantly enhanced invasiveness of ErbB3WT cells into Matrigel, while invasiveness of ErbB3-Mutant cells was significantly lower (Figure 1D). In summary, these data suggest that PI3K association with ErbB3 is required for HRGβ1 to induce chemotaxis and invasion.

The PI3K binding sites are required for enhancement of spontaneous metastatic potential, intravasation and lung seeding

We then investigated the metastatic potential of the three tumor cell lines. Cells were injected into the mammary fat pads of SCID mice. We observed no significant differences in tumor growth and final tumor volumes between the three tumor types (Figure 2A). TUNEL (for apoptotic cells), IBA-1 (for macrophages), pAKT, and pERK staining did not show any differences between the tumors (Supplementary Figures 2 A - D). Strikingly, intravasation as measured by the number of circulating tumor cells was significantly higher for ErbB3WT compared to both pLXSN and ErbB3-Mutant (Figure 2B). However, staining for CD34 revealed that this result was not due to obvious differences in the number of blood vessels, which were the same in all tumor types (Supplementary Figures 2 E and F). Our results indicate that the enhancement in intravasation produced by ErbB3 is dependent upon coupling to PI3K.

Intravasation can be a rate limiting step for metastasis (Wyckoff et al., 2000), and to test whether metastatic capability correlated with intravasation capability, H&E sections of the lungs of the mice were evaluated. The lungs of mice carrying ErbB3WT tumors showed greater than 10 times more metastases than the lungs of mice with pLXSN or ErbB3-Mutant tumors (Figure 2C). These results are consistent with intravasation rates regulating metastasis rates in this model. To evaluate lung seeding ability separately from intravasation efficiency, the three cell lines were injected into the lateral tail vein of SCID mice (experimental metastasis assay). Two weeks post- injection the mice were sacrificed and H&E sections of the lungs were examined for metastases. The lungs of mice injected with ErbB3WT cells had a small, but significant increase (approximately 2-fold) in lung seeding efficiency compared to the lungs of mice injected with the pLXSN and ErbB3-Mutant lines (Figure 2D). We conclude that the PI3-kinase binding sites are required *in vivo* for ErbB3 enhancement of intravasation and lung seeding, with a major contribution to metastasis occurring at the intravasation step.

PI3-kinase binding sites are required for ErbB3 enhancement of *in vivo* motility and invasion

To examine the importance of ErbB3/PI3K for invasion in the primary tumor microenvironment, we used multiphoton microscopy to perform intravital imaging. Intravital imaging enables visualization and quantification of the movement and orientation of fluorescent cells directly at the primary tumor without exogenously added stimulants or chemoattractants. Local motility and invasion in the primary tumor may contribute to the ability of tumor cells to locate blood vessels and to intravasate. GFP expressing lines were used in this assay, and 33-38 days post injection into the mammary fat pad, animals were anesthetized and skin flap surgery was performed to expose the primary tumors for imaging (Wyckoff et al., 2007). Total tumor cell motility in pLXSN, ErbB3WT and ErbB3-Mutant tumors was evaluated by analyzing multiple 30-minute z-series from 7-8 tumors generated from each cell line. We found that ErbB3WT expression significantly enhanced tumor cell motility compared to the pLXSN control (Figure 3A and Supplementary Movies 1 and 2). Importantly, expression of the ErbB3-Mutant did not enhance cell motility above the level of the control cell line.

The ErbB3WT cells were more polarized near vascular and stromal areas in the tumor compared to ErbB3-Mutant cells. We used the length/width ratio of cells in the proximity of vessels to quantify polarization (Wyckoff et al., 2000). There was a significant increase in the length/width ratio in ErbB3WT tumors (Figure 3B). This is consistent with increased sensitivity to endogenous gradients of ligands which could enhance both invasion and intravasation. We evaluated whether there was enhanced invasion *in vivo* in response to HRGβ1 using microneedles containing Matrigel and HRGβ1 inserted into the primary tumors to collect invasive cells (Figure 3C). ErbB3 expression had no effect on basal invasion into needles containing Matrigel alone. However, ErbB3WT tumor cells showed significantly enhanced *in vivo* invasion in response to 50 nM HRGβ1 over the empty vector control, while the mutant cells behaved like control cells. These data reveal that the ability of ErbB3 to directly couple to the PI3K pathway is essential for HRGβ1's ability to stimulate *in vivo* invasion. To model the *in vivo* intravasation step, we used an *in vitro* transendothelial migration (TEM) assay (Figure 3D). Tumor cells alone, or mixed with macrophages, were plated on top of an endothelial monolayer and allowed to migrate through to the other side for 18 hours. For all lines, very few carcinoma cells traversed the endothelium in the absence of macrophages. The addition of macrophages dramatically enhanced the ability of ErbB3WT cells to cross the endothelium, but did not increase the ability of pLXSN to cross. The ErbB3-Mutant line showed enhancement by macrophages which was, however, significantly less than ErbB3WT cells. This is similar to the pattern of intravasation efficiency that we observed *in vivo* (Figure 2B). Importantly, IBA-1 staining of primary tumors revealed the presence of macrophages in all three tumor types (Supplementary Figure 2B), indicating that the defect in intravasation is not due to a difference in macrophage density in the tumor.

PI3-kinase inhibition reduces ErbB3WT chemotaxis, *in vivo* invasion and *in vivo* tumor cell motility

As an independent confirmation of the role of PI3-kinase in chemotaxis and invasion of ErbB3WT cells, we used a p110α-selective PI3-K inhibitor, PIK-75. At a concentration of 200 nM, PIK-75 dramatically reduced the *in vitro* chemotactic response to HRGβ1 (Figure 4A) and lowered pAkt levels by ~40% (Supplementary Figure 3). PI3K inhibition increased Erk activity by ~50%, consistently with a previously observed relief of feed-back inhibition following blockade of the PI3K/Akt pathway (Chandarlapaty et al., 2011; Serra et al., 2011). We then evaluated the effect of PIK-75 on invasion *in vivo*. Comparing microneedles containing HRGβ1 alone or HRGβ1 with PIK-75 inserted into ErbB3WT tumors, significantly fewer ErbB3WT cells migrated into microneedles containing HRGβ1 with PIK-75 compared to HRGβ1 alone (Figure 4B). Of note, a 4-hour treatment of cells *in vitro* with PIK-75 had no effect of cell viability (data not shown). We also examined the ability of systemic PIK-75 to inhibit HRGβ1-induced responses at the primary tumor. Mice bearing ErbB3WT tumors were IP-injected with PIK-75 three hours before performing the *in vivo* invasion assay using microneedles containing HRGβ1. Tumors in PIK-75-treated animals showed significantly reduced *in vivo* invasion (Figure 4C), compared to tumors from vehicle control treated animals confirming the importance of the PI3K pathway in HRGβ1-induced responses *in vivo*. Interestingly, PIK-75 did not inhibit EGF-induced *in vivo* invasion

(Supplementary Figure 4), supporting our hypothesis that PI3K signaling is specifically critical in HRGβ1/ErbB3-driven invasion.

Next we used the same treatment regimen and evaluated tumor cell motility by intravital imaging. PIK-75 treatment significantly reduced total tumor cell motility in ErbB3WT primary tumors (Figure 4D, also see Supplementary Movies 3 and 4). We observed that the ErbB3WT cells treated with vehicle control were more polarized near vessels in the tumor, as compared to tumor cells in mice pretreated with PIK-75. To determine whether this observation was significant, we evaluated the length/width ratio of cells in close proximity to vessels employing the same method used previously to compare the polarization of ErbB3WT and ErbB3-Mutant tumor cells. There was a significant decrease in the length/width ratio in ErbB3 tumors pretreated with the inhibitor (Figure 4E). These effects were not due to differences in tumor cell survival, as TUNEL staining was similar in PIK-75 and vehicle-treated ErbB3WT tumors (data not shown).

Analysis of HRGβ1-induced signaling in the ErbB3 WT and ErbB3 Mutant cells

To provide more mechanistic insight into the pathways that are important for motility and invasion, activity of the PI3K/Akt and the Erk pathways were measured in response to HRGβ1 treatment using phospho-specific antibodies. Cultures were stimulated with HRGβ1 for various times and pAkt (T308) and pERK levels were measured in lysates from the three cell lines. There were no significant differences in the basal levels of pERK, or in the HRGβ1-induced pERK levels in the three cell lines (Figure 5A), In contrast, basal pAKT levels were lower and the kinetics of HRGβ1-induced Akt activation were delayed in the ErbB3-Mutant cells in comparison to the other cell lines. ErbB3WT cells showed maximum pAKT levels by 5 min (Figure 5B and Supplementary Figure 5), while the ErbB3 mutant cells required 10-15 min to reach maximum.

We next examined whether the differential effect on signaling in ErbB3WT and ErbB3-Mutant cells was specific to HRGβ1 stimulation, by evaluating pAKT and pERK after stimulation with EGF (Figure 5 C and D), PDGF or with IGF-1 (Figure 5D). The results show that there was no difference in pAKT or pERK levels in EGF treated cells. IGF-1 caused an increase in pAKT, not pERK, and the pAKT levels were the same in both cell lines. Finally, PDGF had no effect on these pathways, likely due to absence of the receptor. Thus loss of the PI3K binding sites on ErbB3 resulted in AKT phosphorylation in response to HRGβ1.

These results suggest that HRGβ1's ability to cause a rapid stimulation of PI3K signaling is important for its biological activity in motility and invasion. Next we employed an *in vitro* invasion assay using Matrigel-coated transwells in combination with specific inhibitors to investigate pathways downstream of ErbB3 in the ErbB3 WT cells (Figure 5E). We found that HRGβ1-induced invasion was totally blocked by inhibition of p110α and Akt. Next we looked at Rac1, which is downstream of PI3K, in the three cell lines. HRGβ1 rapidly stimulated Rac1 activity by 2-fold in the ErbB3 WT cells, while there was no induction in control and low levels in ErbB3-Mutant cells (Supplementary Figure 6). In accordance with these results treatment with a Rac 1 inhibitor (NSC23766) reduced invasion by approximately 50% (Figure 5E). In contrast, treatment with a Pak inhibitor had no effect on

HRGβ1-induced invasion (data not shown). Taken together, the data suggest that invasion of the ErbB3 WT cells is mainly dependent upon the PI3K-Akt-Rac pathway.

DISCUSSION

In this study we utilized the MTLn3 cell line to evaluate the role of the YXXM sites in ErbB3 in breast cancer metastasis. We find that these sites are required for ErbB3-mediated chemotactic responses to HRGβ1 *in vitro* and invasion responses both *in vitro* and *in vivo*. Increased expression of wild-type ErbB3 had no effect on primary tumor growth, but significantly enhanced intravasation and spontaneous metastasis (Fig 2 and our previous publication (Xue et al., 2006)). Mutation of the YXXM sites dramatically reduced the enhancement of intravasation and metastasis, while having no effect on primary tumor growth. In an experimental metastasis assay, wild-type ErbB3 overexpression had a significant, albeit slight, effect on the lung seeding process, which also required ErbB3 coupling to PI3K. Similarly, an increase in spontaneous motility and cell polarization in the primary tumor induced by wild-type ErbB3 required the YXXM sites. Treatment of tumor-bearing mice with the p110alpha inhibitor PIK-75 caused a significant decrease in intravital motility and *in vivo* invasion, attesting to the important role of PI3K in invasion. Overexpression of ErbB3 in the aggressive MDA-MB-231 human breast cancer model also significantly enhanced the invasiveness of the cells in response to HRGβ1 treatment (Supplementary Figure 7). Taken together the data presented here indicate that the ability of ErbB3 to couple to the PI3K/Akt pathway confers tumors overexpressing this receptor with an enhanced ability to invade and to metastasize.

Based on the studies reported here, we have identified intravasation as a key stage in metastasis that is enhanced by ErbB3 signaling both *in vivo* and in the *in vitro* transendothelial migration assay. Intriguingly, EGFR overexpression is not equivalent to ErbB3 overexpression in the *in vitro* TEM assay, since the former do not show increased intravasation (data not shown), while as we show here ErbB3 overexpression has a positive impact. These results are consistent with our *in vivo* studies using EGFR inhibitors (Kedrin et al., 2009a), where we show that inhibition of EGFR had a slow inhibitory effect on intravasation and was only evident with a delay of several hours after EGFR inhibition. Conversely, inhibition of ErbB2 rapidly inhibited intravasation (Kedrin et al., 2009b). Since ErbB3 forms preferred heterodimers with ErbB2, this suggests that an ErbB3/ErbB2 heterodimer is important in enhancing the intravasation step, while EGFR is important for tumor cell invasion from the primary tumor to reach the blood vessels (Kedrin et al., 2009a). HRGβ1 is present in serum in subnanomolar concentrations (Ky et al., 2009), and by increasing ErbB3 levels in the tumor cells this might enable them to detect low levels of HRGβ1 and increase their intravasation. Endothelial cells have also been reported to express HRGβ1, which may also stimulate intravasation (Iivanainen et al., 2007; Kalinowski et al.).

HRGβ1 activated PI3K/Akt in both ErbB3 WT and ErbB3-Mutant cells but with different kinetics. In ErbB3WT cells the pathway was maximally activated after 5min of HRGβ1 stimulation, while it took between 10 and 15min to see the same signal intensity in the ErbB3-Mutant cells. This suggests that early pathway activation, which is dependent upon p85/PI3K binding to HRGβ1 activated ErbB3-containing heterodimers, is responsible for the

major effects of the ligand on migration and invasion. The fact that blockade of PI3K or Akt activity using selective inhibitors totally blocked HRGβ1-induced invasion (Fig 5E), while ErbB3-Mutant cells were only blocked in their invasive ability by ~ 60% (Fig 1D), very likely reflects the fact that the PI3K/Akt pathway does get activated in these cells, but with slower kinetics. The importance of the kinetics of signaling pathway activation in response to ErbB ligands has been observed in other systems, (see, e.g. (Olayioye et al., 2001)).

While previous studies have shown the direct binding of p85 and subsequent signaling from all six YXXM motifs on the ErbB3 C-terminus (Hellyer et al., 2001; Prigent and Gullick, 1994), high-throughput methods such as protein microarray studies suggest that other molecules could bind these sites (Jones et al., 2006). To confirm that the phenotype in the ErbB3-Mutant MTLn3 cells is due to defective PI3K pathway signaling, we used the p110-α selective inhibitor PIK-75, revealing that the *in vitro* chemotaxis as well as *in vivo* invasion of MTLn3-ErbB3WT cells towards HRGβ1 was impaired following PI3K inhibition. Moreover pretreatment of mice carrying ErbB3WT cell-induced tumors with PIK-75 caused reduced tumor cell motility, as visualized by multiphoton microscopy. Furthermore, the cells in the treated tumors were also more rounded on average as quantified by length/width ratios, thus mimicking the phenotype of the mutant ErbB3 tumors. These experiments support the hypothesis that PI3K pathway activation by ErbB3 is a major contributor to enhancing the initial steps of the metastatic cascade of mammary tumor cells.

MATERIALS and METHODS

Cell culture

Rat mammary carcinoma MTLn3 cells (Neri et al., 1982) were grown in α-MEM supplemented with 5% fetal bovine serum (FBS) and penicillin/streptomycin solution (Life Technologies). HRGβ1 was from R & D Systems (396-HB). MDA-MB-231 cells (American Type Culture Collection) were cultured in DMEM (Invitrogen) with 10% fetal bovine serum.

Animal models and in vivo assays for metastatic progression

All procedures involving mice were conducted in accordance with the National Institutes of Health regulations concerning the use and care of experimental animals. The study of mice was approved by the Albert Einstein College of Medicine animal use committee. MTLn3 derived cell lines were grown to 70-85% confluence before being harvested for in vivo assays. To measure spontaneous metastasis, 5×10^5 cells were detached by incubation in DPBS + 2 mmol/L EDTA, scraping with a rubber policeman, centrifuged, and resuspended in DPBS at 10^7 cells/mL. MTLn3 (5×10^5) cells were injected into the right fourth mammary fat pad from the head of 5- to 7-week-old female severe combined immunodeficient (SCID/NCr) mice (National Cancer Institute, Bethesda, MD) in 100 μL DPBS with calcium and magnesium (Mediatech 21-031-cv) through a 25-gauge needle. Tumor growth rate was monitored at weekly intervals by measuring in two dimensions, and tumor volumes were calculated using the formula: length $\times$ width^2/2. At the end point for spontaneous metastasis, the blood burden assay was performed using blood taken from the right atrium via heart puncture with a 25-gauge needle and a 1 mL syringe coated with

heparin and containing 0.1 mL of heparin. Blood was plated in tissue culture medium and after 7 days all tumor colonies in the dish were counted. Tumor blood burden was calculated as the total colonies in the dish divided by the volume of blood taken. To measure experimental lung metastasis, 5×10^5 cells were injected into the lateral tail veins of 5- to 7-week-old female SCID mice (National Cancer Institute). Two weeks after injection, the mice were sacrificed, and the lungs were removed, fixed in formalin, and stained H&E sections were counted for metastasis. For each lung sample, all micrometastases were counted using a 10x objective. The efficiency of lung metastasis was expressed in number of metastases per lung section for each animal. Mean and SE were then calculated for each cell line.

In Vivo Invasion assay

The measurement of cell invasion into needles placed in the primary tumor of anesthetized mice was carried out as described previously in detail (Hernandez et al., 2009b). Invasive cells were collected into 33-gauge Hamilton needles (Fisher 14-815-423) filled with Matrigel (Beckton Dickinson 356234) diluted 1:10 with L15-BSA +/- chemoattractant for 4 hours. At the end of collection, the contents of the needles were extruded using 0.5 μg/ml DAPI in PBS in a syringe onto a coverslip. The chemoattractants used in this assay include HRGβ1 at a concentration of 50 nM (R & D Systems 396-HB) and EGF at 25 nM (Life Technologies). To inhibit the activity of PI3-kinase, PIK-75 (Axon Medchem, Axon 1334), a p110-alpha-selective inhibitor (Chaussade et al., 2007), was used at 1 μM.

Intravital Imaging

Orthotopic primary tumors were grown and imaged at 4-5 weeks post injection. The animal was anesthetized, and a skin flap surgery was performed to expose the tumor. The animal was placed on an inverted microscope and tumor cells were imaged using a Radiance 2000 MP multiphoton or on an Olympus Fluoview FV1000-MPE microscope using an excitation wavelength of 880nm with a 20X 0.95NA water objective (Wyckoff et al., 2007) or a 25X 1.05NA water objective at resolutions of 1.06 and 0.994 um per pixel, respectively. Cell motility was observed by time-lapse imaging over 30 min at 2-minute intervals, where a 100 μm z-series, with 10 μm steps, was collected at each time point. For quantification of average total cell motility, a motility event was defined as a protrusion of half a cell length or more. The length/width ratio (L/W) was calculated using ImageJ as follows: length was scored as the Feret's diameter of the cell (the longest distance between any two points along the boundary); width was scored as the secondary axis of the best fit ellipse of the circled cells. Cells near stromal and vascular areas of the tumor in the top 40 um from the tumor surface were selected for these measurements. For inhibition of PI3-kinase in the tumor cells *in vivo* for imaging, PIK-75 was dissolved in DMSO and three hours prior to imaging, a dose calculated to be 50mg/kg of body mass was mixed with 200-300 ul PBS such that the final solution consisted of no more than 20% DMSO and 20% β-cyclodextrin, and injected intraperitoneally, following a previously described procedure (Hayakawa et al., 2007).

Additional reagents and methods are described in the Supplementary Materials and Methods.

Statistical Analysis

Statistical significance was determined using unpaired, two-tailed Student's t tests assuming unequal variances and an alpha level of 0.05. Differences were considered significant if the p value was <0.05. For blood burden assays the non-parametric Mann Whitney Wilcoxon rank sum test was used.

Supplementary Material

Refer to Web version on PubMed Central for supplementary material.

Acknowledgments

References

Adam L, Vadlamudi R, Kondapaka SB, Chernoff J, Mendelsohn J, Kumar R. Heregulin regulates cytoskeletal reorganization and cell migration through the p21-activated kinase-1 via phosphatidylinositol-3 kinase. J Biol Chem. 1998; 273:28238–28246. [PubMed: 9774445]

Amin DN, Campbell MR, Moasser MM. The role of HER3, the unpretentious member of the HER family, in cancer biology and cancer therapeutics. Semin Cell Dev Biol.

Baselga J, Swain SM. Novel anticancer targets: revisiting ERBB2 and discovering ERBB3. Nat Rev Cancer. 2009; 9:463–475. [PubMed: 19536107]

Burgess AW. EGFR family: structure physiology signalling and therapeutic targets. Growth Factors. 2008; 26:263–274. [PubMed: 18800267]

Cain RJ, Ridley AJ. Phosphoinositide 3-kinases in cell migration. Biol Cell. 2009; 101:13–29. [PubMed: 19055486]

Campbell MR, Amin D, Moasser MM. HER3 comes of age: new insights into its functions and role in signaling, tumor biology, and cancer therapy. Clin Cancer Res. 2010; 16:1373–1383. [PubMed: 20179223]

Chandarlapaty S, Sawai A, Scaltriti M, Rodrik-Outmezguine V, Grbovic-Huezo O, Serra V, Majumder PK, Baselga J, Rosen N. AKT inhibition relieves feedback suppression of receptor tyrosine kinase expression and activity. Cancer Cell. 2011; 19:58–71. [PubMed: 21215704]

Chausovsky A, Waterman H, Elbaum M, Yarden Y, Geiger B, Bershadsky AD. Molecular requirements for the effect of neuregulin on cell spreading, motility and colony organization. Oncogene. 2000; 19:878–888. [PubMed: 10702796]

Chaussade C, Rewcastle GW, Kendall JD, Denny WA, Cho K, Gronning LM, Chong ML, Anagnostou SH, Jackson SP, Daniele N, Shepherd PR. Evidence for functional redundancy of class IA PI3K isoforms in insulin signalling. Biochem J. 2007; 404:449–458. [PubMed: 17362206]

Chiu CG, Masoudi H, Leung S, Voduc DK, Gilks B, Huntsman DG, Wiseman SM. HER-3 Overexpression Is Prognostic of Reduced Breast Cancer Survival: A Study of 4046 Patients. Annals of Surgery. 251:1107–1116. 1110.1097/SLA.1100b1013e3181dbb1177e. [PubMed: 20485140]

Di Cosimo S, Baselga J. Management of breast cancer with targeted agents: importance of heterogeneity. [corrected]. Nat Rev Clin Oncol. 2010; 7:139–147. [PubMed: 20125090]

Engelman JA, Janne PA, Mermel C, Pearlberg J, Mukohara T, Fleet C, Cichowski K, Johnson BE, Cantley LC. ErbB-3 mediates phosphoinositide 3-kinase activity in gefitinib-sensitive non-small cell lung cancer cell lines. Proc Natl Acad Sci U S A. 2005; 102:3788–3793. [PubMed: 15731348]

Engelman JA, Zejnullahu K, Mitsudomi T, Song Y, Hyland C, Park JO, Lindeman N, Gale CM, Zhao X, Christensen J, et al. MET amplification leads to gefitinib resistance in lung cancer by activating ERBB3 signaling. Science. 2007; 316:1039–1043. [PubMed: 17463250]

Fiddes RJ, Campbell DH, Janes PW, Sivertsen SP, Sasaki H, Wallasch C, Daly RJ. Analysis of Grb7 recruitment by heregulin-activated erbB receptors reveals a novel target selectivity for erbB3. J Biol Chem. 1998; 273:7717–7724. [PubMed: 9516479]

Fujimoto N, Wislez M, Zhang J, Iwanaga K, Dackor J, Hanna AE, Kalyankrishna S, Cody DD, Price RE, Sato M, et al. High expression of ErbB family members and their ligands in lung adenocarcinomas that are sensitive to inhibition of epidermal growth factor receptor. Cancer Res. 2005; 65:11478–11485. [PubMed: 16357156]

Hayakawa M, Kawaguchi K, Kaizawa H, Koizumi T, Ohishi T, Yamano M, Okada M, Ohta M, Tsukamoto S, Raynaud FI, et al. Synthesis and biological evaluation of sulfonylhydrazone-substituted imidazo[1,2-a]pyridines as novel PI3 kinase p110alpha inhibitors. Bioorg Med Chem. 2007; 15:5837–5844. [PubMed: 17601739]

Hellyer NJ, Kim MS, Koland JG. Heregulin-dependent activation of phosphoinositide 3-kinase and Akt via the ErbB2/ErbB3 co-receptor. J Biol Chem. 2001; 276:42153–42161. [PubMed: 11546794]

Hernandez L, Smirnova T, Kedrin D, Wyckoff J, Zhu L, Stanley ER, Cox D, Muller WJ, Pollard JW, Van Rooijen N, Segall JE. The EGF/CSF-1 paracrine invasion loop can be triggered by heregulin beta1 and CXCL12. Cancer Res. 2009a; 69:3221–3227. [PubMed: 19293185]

Hernandez L, Smirnova T, Wyckoff J, Condeelis J, Segall JE. In vivo assay for tumor cell invasion. Methods Mol Biol. 2009b; 571:227–238. [PubMed: 19763970]

Holbro T, Beerli RR, Maurer F, Koziczak M, Barbas CF 3rd, Hynes NE. The ErbB2/ErbB3 heterodimer functions as an oncogenic unit: ErbB2 requires ErbB3 to drive breast tumor cell proliferation. Proc Natl Acad Sci U S A. 2003; 100:8933–8938. [PubMed: 12853564]

Iivanainen E, Paatero I, Heikkinen SM, Junttila TT, Cao R, Klint P, Jaakkola PM, Cao Y, Elenius K. Intra- and extracellular signaling by endothelial neuregulin-1. Exp Cell Res. 2007; 313:2896–2909. [PubMed: 17499242]

Jones RB, Gordus A, Krall JA, MacBeath G. A quantitative protein interaction network for the ErbB receptors using protein microarrays. Nature. 2006; 439:168–174. [PubMed: 16273093]

Kalinowski A, Plowes NJ, Huang Q, Berdejo-Izquierdo C, Russell RR, Russell KS. Metalloproteinase-dependent cleavage of neuregulin and autocrine stimulation of vascular endothelial cells. FASEB J. 24:2567–2575. [PubMed: 20215529]

Kedrin D, Wyckoff J, Boimel PJ, Coniglio SJ, Hynes NE, Arteaga CL, Segall JE. ERBB1 and ERBB2 have distinct functions in tumor cell invasion and intravasation. Clin Cancer Res. 2009a; 15:3733–3739. [PubMed: 19458057]

Kedrin D, Wyckoff J, Boimel PJ, Coniglio SJ, Hynes NE, Arteaga CL, Segall JE. ERBB1 and ERBB2 have distinct functions in tumor cell invasion and intravasation. Clin Cancer Res. 2009b; 15:3733–3739. [PubMed: 19458057]

Ky B, Kimmel SE, Safa RN, Putt ME, Sweitzer NK, Fang JC, Sawyer DB, Cappola TP. Neuregulin-1 beta is associated with disease severity and adverse outcomes in chronic heart failure. Circulation. 2009; 120:310–317. [PubMed: 19597049]

Neri A, Welch D, Kawaguchi T, Nicolson GL. Development and biologic properties of malignant cell sublines and clones of a spontaneously metastasizing rat mammary adenocarcinoma. J Natl Cancer Inst. 1982; 68:507–517. [PubMed: 6950180]

Olayioye MA, Badache A, Daly JM, Hynes NE. An essential role for Src kinase in ErbB receptor signaling through the MAPK pathway. Exp Cell Res. 2001; 267:81–87. [PubMed: 11412040]

Prigent SA, Gullick WJ. Identification of c-erbB-3 binding sites for phosphatidylinositol 3'-kinase and SHC using an EGF receptor/c-erbB-3 chimera. Embo J. 1994; 13:2831–2841. [PubMed: 8026468]

Sassen A, Rochon J, Wild P, Hartmann A, Hofstaedter F, Schwarz S, Brockhoff G. Cytogenetic analysis of HER1/EGFR, HER2, HER3 and HER4 in 278 breast cancer patients. Breast Cancer Res. 2008; 10:R2. [PubMed: 18182100]

Schade B, Lam SH, Cernea D, Sanguin-Gendreau V, Cardiff RD, Jung BL, Hallett M, Muller WJ. Distinct ErbB-2 coupled signaling pathways promote mammary tumors with unique pathologic and transcriptional profiles. Cancer Res. 2007; 67:7579–7588. [PubMed: 17699761]

Serra V, Scaltriti M, Prudkin L, Eichhorn PJ, Ibrahim YH, Chandarlapaty S, Markman B, Rodriguez O, Guzman M, Rodriguez S, et al. PI3K inhibition results in enhanced HER signaling and acquired ERK dependency in HER2-overexpressing breast cancer. Oncogene. 2011

Siegel PM, Ryan ED, Cardiff RD, Muller WJ. Elevated expression of activated forms of Neu/ErbB-2 and ErbB-3 are involved in the induction of mammary tumors in transgenic mice: implications for human breast cancer. EMBO J. 1999; 18:2149–2164. [PubMed: 10205169]

Vijapurkar U, Kim MS, Koland JG. Roles of mitogen-activated protein kinase and phosphoinositide 3'-kinase in ErbB2/ErbB3 coreceptor-mediated heregulin signaling. Exp Cell Res. 2003; 284:291–302. [PubMed: 12651161]

Wyckoff JB, Jones JG, Condeelis JS, Segall JE. A critical step in metastasis: in vivo analysis of intravasation at the primary tumor. Cancer Res. 2000; 60:2504–2511. [PubMed: 10811132]

Wyckoff JB, Wang Y, Lin EY, Li JF, Goswami S, Stanley ER, Segall JE, Pollard JW, Condeelis J. Direct visualization of macrophage-assisted tumor cell intravasation in mammary tumors. Cancer Res. 2007; 67:2649–2656. [PubMed: 17363585]

Xue C, Liang F, Mahmood R, Vuolo M, Wyckoff J, Qian H, Tsai KL, Kim M, Locker J, Zhang ZY, Segall JE. ErbB3-dependent motility and intravasation in breast cancer metastasis. Cancer Res. 2006; 66:1418–1426. [PubMed: 16452197]

Zhang J, Zhong W, Cui T, Yang M, Hu X, Xu K, Xie C, Xue C, Gibbons GH, Liu C, et al. Generation of an adult smooth muscle cell-targeted Cre recombinase mouse model. Arterioscler Thromb Vasc Biol. 2006; 26:e23–24. [PubMed: 16484601]
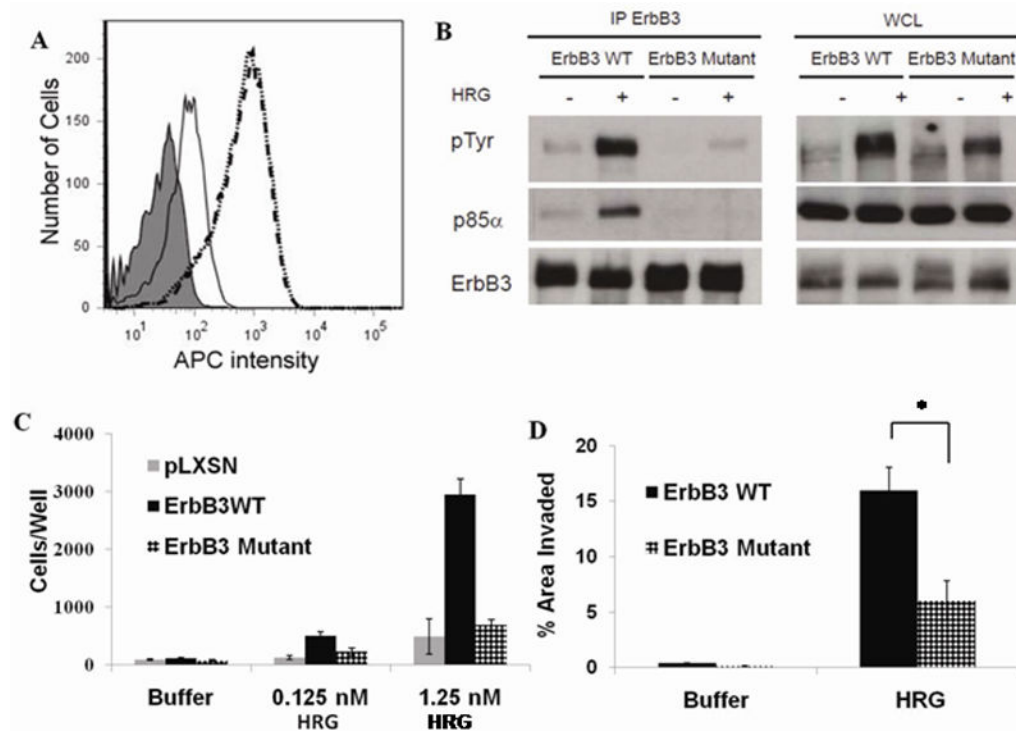
Figure 1. ErbB3 mutations block tyrosine phosphorylation, PI3K binding and show a defect in *in vitro* chemotaxis and invasion to HRGβ1

A. Flow cytometry analysis of surface ErbB3 levels in pLXSN (solid line), ErbB3WT (dotted line), and ErbB3-Mutant (dashed line) cells. A mouse anti-ErbB3 primary followed by an APC-labeled secondary was used. The curve with solid shading represents ErbB3WT cells incubated with just the APC-conjugated secondary antibody.

B. HRGβ1-induced ErbB3 tyrosine phosphorylation and association to the p85 subunit of PI3K. Serum starved MTLn3 ErbB3WT or ErbB3-Mutant cells were stimulated with buffer or HRGβ1 (0 or 0.4 HRG) for 5 minutes. ErbB3 immunoprecipitates (IP) and whole cell lysates (WCL) were resolved by SDS/PAGE, and probed for (PTyr) or p85α. Membranes were stripped and reprobed to control for ErbB3 levels.

C Chemotaxis to HRGβ1 of pLXSN (light gray bars), ErbB3WT (dark gray bars) and ErbB3-Mutant (patterned bars). Data are mean and SEM of 6-27 wells in 3-6 independent experiments.

D. *In vitro* invasion responses of ErbB3WT (black bars) and ErbB3-Mutant cells (patterned bar) into Matrigel-coated transwells stimulated by buffer or 12.5 nM HRGβ1. Data are presented as % Area invaded, and are mean and SEM of 3 independent experiments. *:p< 0.02
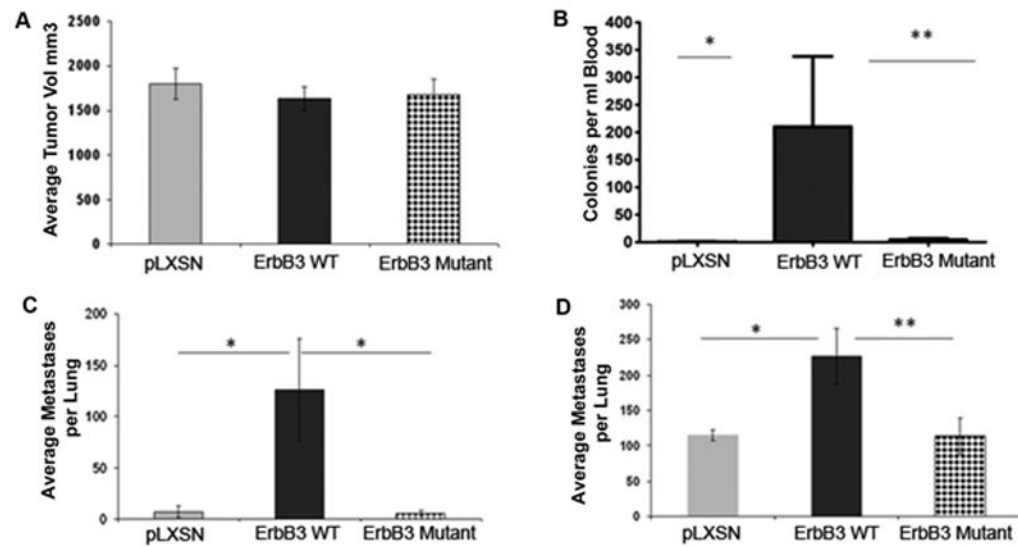
Figure 2. PI3-kinase binding sites contribute to intravasation and lung metastasis
A. Tumor growth after orthotopic injection into the mammary fat pad. There are no statistically significant differences between the average primary tumor volumes formed by MTLn3 pLXSN, ErbB3WT or ErbB3-Mutant lines. Data are means and SEM of 9-27 tumor measurements determined on average 36 days after injection for all cell lines.
B. Intravasation measured 4-5 weeks post injection into the mammary fat pad. Blood drawn from the right atrium of the heart was plated into cell culture medium and colonies were counted 7 days later. Data are means and SEM of total numbers of colonies normalized per ml of blood drawn for 15 – 17 mice per cell line. *: p<0.004, **: p<0.05.
C. Spontaneous metastatic potential measured 4-5 weeks post injection into the mammary fat pad was determined by quantifying metastases in H&E stained sections through the middle of the lungs. Data are means and SEM of counts from 11 – 13 animals carrying tumors from each cell line. *: p< 0.02
D. Lung seeding efficiency determined by evaluating metastases in H&E stained sections through the middle of the lungs 2 weeks post injection via tail vein. Data are means and SEM of 9 – 12 animals per cell line. *: p<0.02, **: p<0.03

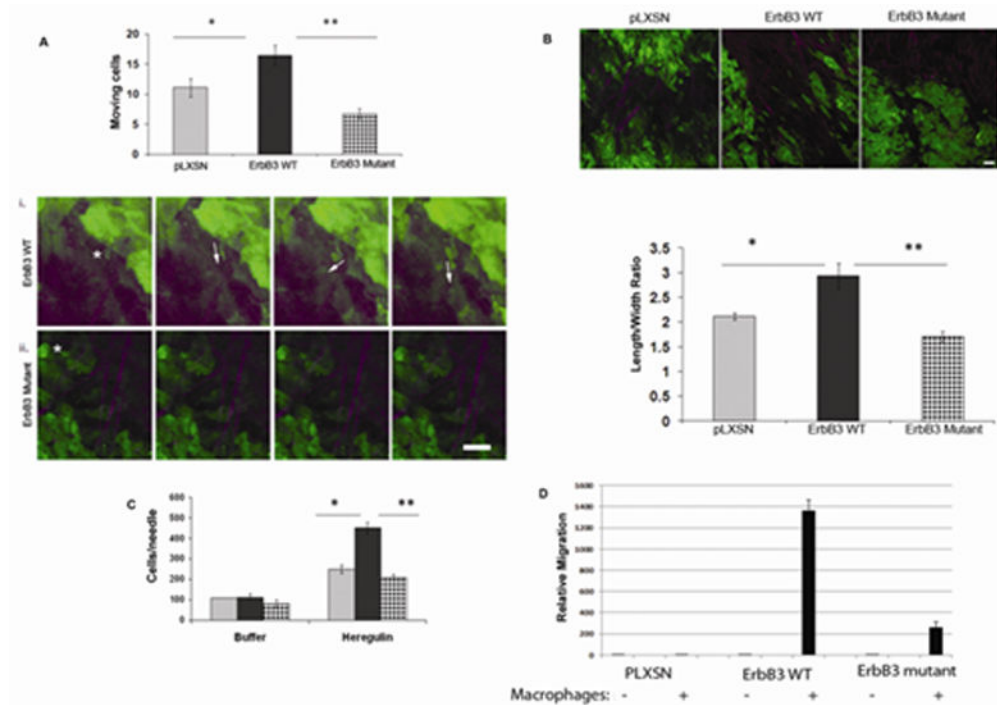Author Manuscript

Author Manuscript

Author Manuscript

Author Manuscript

Figure 3. PI3-kinase binding sites are required for ErbB3 enhancement of *in vivo* motility and invasion

A. Intravital imaging using multiphoton microscopy of primary mammary tumors of GFP-labeled tumor cells. Time-lapse z-series were acquired and the average total cell motility was determined per 40 μm z-stack (5 sections imaged at 10 μm intervals). Data are means and SEM of 24 – 33 separate z stacks from 7-8 mice per cell line. *: p<0.025, **: p<0.0000042. i/ii panels illustrate examples of (i) ErbB3WT GFP and (ii) ErbB3-Mutant GFP cell motility *in vivo*. Cells are green with collagen fibers detected by second harmonic scattering in purple. Frames are 6 minutes apart, arrows show migrating tumor cell; Scale bar = 25 μm. Asterisks mark a single cell in i and ii and arrows mark a moving cell in i.

B. Length/width ratio comparisons. **Top**: representative images. **Bottom:** Mean and SEM of ratios of 50-100 cells from 3 tumors, 5 slices analyzed per z stack. Scale bar = 25 μm. *: p<0.002, **: p<6×10^{-5}

C. *In vivo* invasion responses. Microneedles containing buffer or 50 nM HRGβ1 were inserted into primary tumors and invasive cells were quantified. *: p<4×10^{-5}, **: p< 5×10^{-6}. Data are means and SEM of 9-13 measurements from 3-4 tumors per cell line (pLXSN: gray, ErbB3WT: black, ErbB3-Mutant: patterned).

D. *In vitro* transendothelial migration assay. Cells were plated on the basal side of an endothelial monolayer either alone or mixed with macrophages (+M) and allowed to migrate for 18 hours. for comparison of ErbB3WT+M with ErbB3-Mutant+M: p<4×10^{-6}. Data are represented as the fold migration over pLXSN alone, with mean and SEM of 4 independent experiments with each cell line.
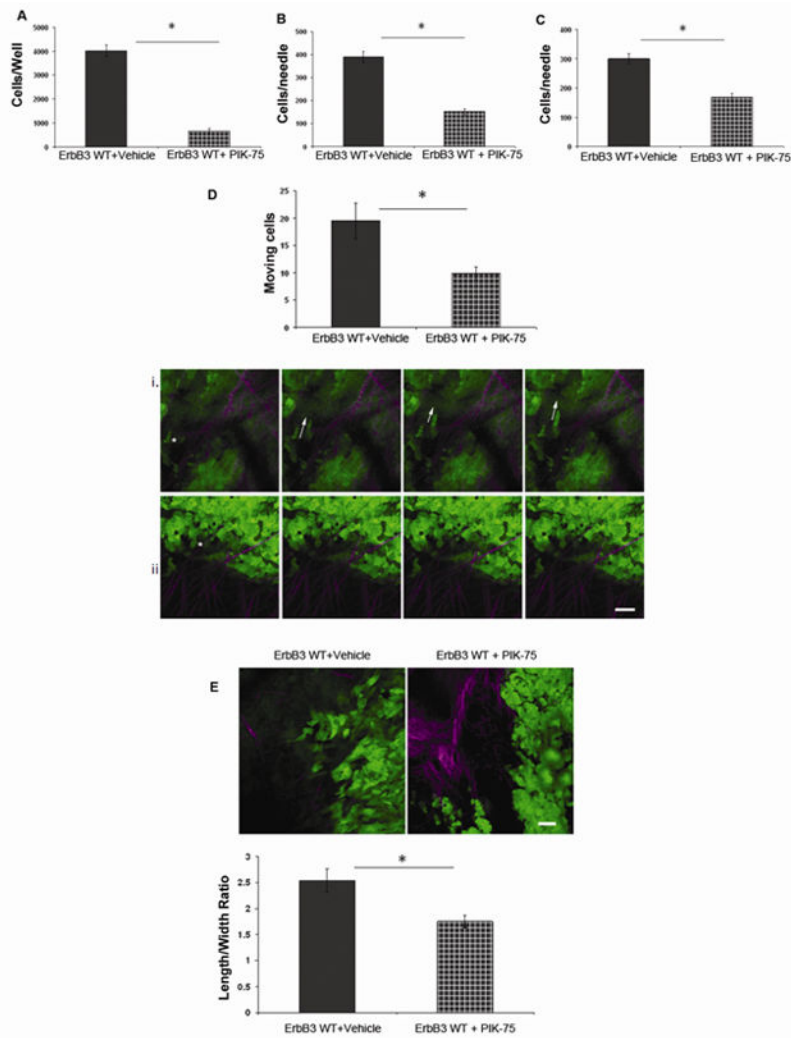
Figure 4. The PI3-kinase inhibitor PIK-75 blocks HRGβ1 induced chemotaxis, in vivo invasion and total tumor cell motility

A. In vitro chemotaxis is inhibited by PIK-75. Migration of ErbB3WT cells in response to a gradient of either 1.25 nM HRGβ1 (black bar) or 1.25 nM HRGβ1 + 0.2 μM PIK-75 (patterned bar). *: p< 0.0001. Data are mean and SEM of measurements from 3 independent experiments.

B. *In vivo* invasion is inhibited by PIK-75. Microneedles containing 50 nM HRGβ1or 50 nM HRGβ1 + 1 μM PIK-75 were inserted into the primary tumor and invasive cells were collected and counted. Data are mean and SEM from 6 needles for HRGβ1 and 10 needles for HRGβ1 + PIK-75 from 3 tumors for each condition. *: p< 1×10^{-5}.

C. *In vivo* invasion stimulated by 50 nM HRGβ1 is inhibited by systemic application of PIK-75. Mice bearing ErbB3WT tumors were injected i.p. either with vehicle control (black bar) or with 1.5 mg PIK-75 (pattern) 3 hours prior to assay. Microneedles containing 50 nM HRGβ1 were inserted into primary tumors and invasive cells were quantified as described in the methods.*: p< 0.00035. Data are means and SEM of 4-8 measurements from 4 tumors per condition.

D. Cell motility *in vivo* using intravital imaging. Mice bearing tumors were injected i.p. either with vehicle control (black bar) or with 1.5 mg PIK-75 (pattern) 3 hours prior to imaging. Tumors were exposed by skin-flap surgery and time-lapse z-series were acquired. The average total cell motility was determined per 40 μm z-stack (5 sections imaged at 10 μm intervals).

Top: Data are means and SEM of 8 (vehicle control) and 15 (PIK-75) separate z stacks from 3 mice per condition. *: p< 0.016

Bottom: Representative panels from tumors of animals injected with (i) MTLn3-ErbB3--GFP vehicle control or (ii) PIK-75 3 hours prior to imaging. Cells are green with collagen fibers detected by second harmonic scattering in purple. Frames are 6 minutes apart, arrow shows migrating tumor cell; * indicates a single cell. Scale bar = 25 μm.

E. Length/width ratio comparison. **Top**: representative images **Bottom:** Mean and SEM of 40-50 cells from 3 tumors per condition, 5 slices analyzed per field. Scale bar = 25 μm.*: p<0.002
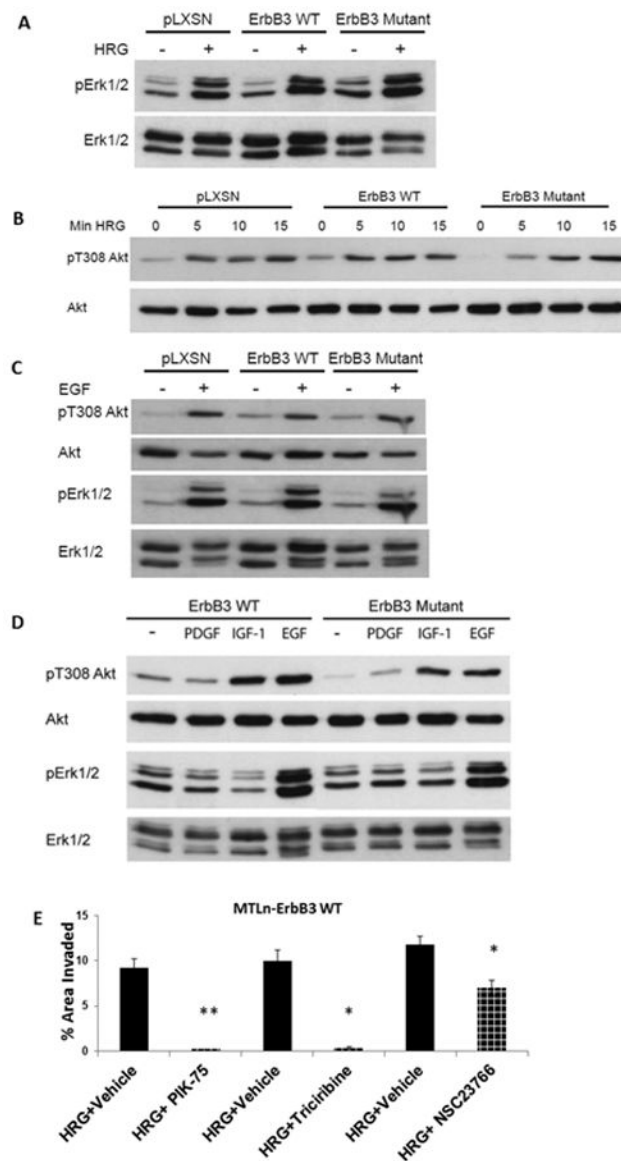
Figure 5. Analysis of HRGβ1 induced signaling in the ErbB3 WT and ErbB3-Mutant cells

A. Erk phosphorylation was determined in serum-starved cells after 5 minute treatment with 0 (-) or 0.4 nM HRGβ1 (+). Similar results were observed in three independent experiments.

B. MTLn3 pLXSN, ErbB3WT, and ErbB3-Mutant cells were stimulated with 0.4 nM HRGβ1for 0, 5, 10, and 15 minutes (Min HRG). A delay in phosphorylation of Akt on Thr 308 was observed in ErbB3-Mutant cells response to HRGβ1.

C. Akt (T308) and Erk phosphorylation activation was determined in serum-starved cells after 5 min treatment with 0 (-) or 5 nM (+) EGF. Similar results were observed in three independent experiments.

D. Akt (T308) and Erk phosphorylation activation was determined in serum-starved cells after 10 min treatment with PDGF, IGF-I, and EGF. Similar results were observed in three independent experiments.

E. Matrigel-coated transwells were used to test 12.5 nM HRGβ1induced *in vitro* invasion responses of MTLn3 ErbB3WT in the presence of vehicle (gray bars) or inhibitor (patterned bars). PIK-75 is a p110α selective inhibitor, Triciribine is an Akt inhibitor, and NSC23766 is a Rac1 inhibitor. Data are mean and SEM from 3 independent experiments. *: p< 0.05, **: p< 1.83E-05